Limnol. Oceanogr., 37(4), 1992, 813–828

Event-scale response of phytoplankton to watershed inputs in a subestuary: Timing, magnitude, and location of blooms

C. L. Gallegos, T. E. Jordan, and D. L. Correll
Smithsonian Environmental Research Center, P.O. Box 28, Edgewater, Maryland 21037

Abstract

Subestuaries receive direct runoff from a local watershed and exchange water at their mouth with a mainstem estuary. For subestuaries close to the headwaters of the mainstem estuary, the potential exists for a single rainfall event to supply nutrients to the subestuary on two time scales corresponding to arrival of flow from the two sources. We present a model of phytoplankton blooms based on the Rhode River-Muddy Creek subestuary of Chesapeake Bay which indicates that nutrient inputs from local sources should be capable of producing blooms of small scale and short duration, whereas influx from the mainstem estuary causes blooms of greater extent. Phytoplankton dynamics were simulated with a modification of models for nutrient-saturated standing crop, in which external nutrient inputs were assumed to favor growth of components of the community that have lower loss rates. Field data for two events during late spring and early summer 1989 demonstrated the initiation of blooms by the arrival of freshwater from local and remote sources. As predicted by the model, blooms initiated by the arrival of remote inputs were of larger spatial extent than those triggered by local inputs.

Aquatic ecosystems are often strongly influenced by linkages to terrestrial ecosystems. For example, Hutchinson (1967) suggested that the terms "eutrophic systems" and "oligotrophic systems" be applied to lakes and their entire drainage basins, rather than to lakes separately. A watershed-ecosystem perspective was also advocated by Likens (1984) and applied extensively in the Hubbard Brook-Mirror Lake system (Likens 1985). Similarly, the river continuum hypothesis (Vannote et al. 1980) predicts that properties of lotic ecosystems vary with increasing stream order as a result of, among other things, reduced impact of the surrounding forest on processes within the stream.

Discerning effects of the watershed on upland aquatic systems is simplified by the downstream directionality of water flow. In coastal plain streams that are tributary to an estuary (i.e. subestuaries), bidirectional tidal flows make such analyses more complicated. In a subestuary there are two inputs of chemical constituents: direct runoff from the local watershed and mixing of water across the downstream boundary with the mainstem estuary.

The effect of water derived from the mainstem will depend on the location of the subestuary along the salinity gradient of the mainstem estuary. Locations near the mouth of the mainstem estuary would be expected to be more closely coupled to continental shelf processes (e.g. Lewis and Platt 1982; Côté and Platt 1983) or tidal forcing (Hayward et al. 1982), whereas those closer to the head of the estuary would receive more influx of materials from the watershed of the mainstem. In the latter case, we might expect that biological processes in a subestuary that depend on the influx of materials of terrestrial origin could display two distinct temporal and spatial scales of response to variations in influx, corresponding to the two distinct sources. That is, inputs from the local watershed respond to localized storms and enter the subestuary at its head. In contrast, the higher order mainstem estuary responds to storms of more regional extent, and the associated inputs enter the subestuary at its mouth. Furthermore, the arrival of inputs from the mainstem is delayed and extended over the time required for flow from all upstream tributaries to reach the mouth of the subestuary.

The impact of freshwater influx on phy-

Acknowledgments

We thank S. Hedrick and J. Miklas for help with collection and analysis of samples, and J. Duls for maintanence of field monitoring sites. R. Magnien provided data from the Chesapeake Bay water quality monitoring program.

This study was supported by the Smithsonian Institution's Environmental Sciences Program and by NSF grants BSR 86-15902 and BSR 89-05210.

toplankton production and biomass in estuaries varies among systems. River flow contains nutrients from weathered soils, municipal sewage, and agricultural sources (Duda 1982; Correll 1978, 1981) that can contribute to accumulation of large standing crops of phytoplankton limited only by self shading (Paerl 1988). Conversely, the suspended particulate load carried in freshwater runoff reduces light penetration and prevents utilization of available nutrients by phytoplankton in some systems (Cloern 1987; Randall and Day 1987). Thus, it is possible to predict spring phytoplankton biomass levels in some estuaries using nutrient-saturated formulations (Pennock 1985). Considering also that a system may be nutrient saturated due to high rates of regeneration, it seems reasonable that nutrient-saturated models might be applied to a system having a wide range of phytoplankton standing crops and that episodic inputs of allochthonous nutrients and turbidity might alter the relative importance of regulating factors.

In an analysis of long-term water-quality data from the Rhode River, Maryland, a eutrophic subestuary on the western shore of Chesapeake Bay, Jordan et al. (1991*b*) found that chlorophyll concentration in the lower subestuary lagged flow from the Susquehanna River (the main freshwater source to the upper Chesapeake Bay) by 2 weeks. This lagged correlation was significant, but rather weak, and occurred only in spring. Correlations between chlorophyll and local flow were weak but negative. Previous results suggested that resolution of the influence of local and remote watershed inputs on phytoplankton populations in a subestuary would require better spatial and temporal resolution in the sampling scheme.

In 1988 we added a sampling program for phytoplankton dynamics in the Rhode River, with finer spatial and temporal resolution, while maintaining the watershed and estuarine water-quality monitoring programs. Spring and summer 1989 were unusually wet for the decade. Several storms produced measurable responses of the phytoplankton community. Here we combine data from these programs and attempt to establish the system's response to individual, episodic inputs of freshwater. We begin with a conceptual model of the response of phytoplankton to episodic nutrient inputs from the local and remote watersheds. Phytoplankton dynamics are modeled with a modification of a previously published (Wofsy 1983) equation for nutrient-saturated biomass in a mixed layer whereby nutrient inputs are assumed to favor an assemblage with lower loss rates. The model illustrates the short-lived and localized nature of the response of the system to local inputs and the possibility that a single large storm may elicit responses on two distinct time scales. Analysis of field data confirms predictions of the model that blooms may result from inputs from both local and mainstem watersheds, but blooms of local origin are shorter lived and thus more difficult to detect.

Conceptual model

Physical representation—We model an idealized subestuary as two well-mixed boxes in series (e.g. Officer 1980; Han 1974; Jordan et al. 1991*a*). The smaller, shallower upstream box receives direct input of runoff from the local watershed and mixes with the deeper, larger downstream box (Fig. 1), which mixes with the mainstem estuary. Boxes are considered to be homogeneous, and mixing rate of a constituent between boxes is assumed to be proportional to the concentration difference. Volumes and depths of the boxes loosely represent three sampling regions of the Rhode River (*see below*).

The volume of the mainstem estuary is considered to be infinite, i.e. outward mixing of water from the downstream box of the subestuary has no influence on concentrations of materials in the mainstem estuary (Loftus et al. 1972). Concentration of nutrients in the inflow from the local watershed is considered to be constant and storm-related inputs are modeled as pulses of increased volumetric flow (liters^3 t^{-1}). In contrast, arrival of storm water from the remote watershed is modeled as a 12-d increase in nutrient concentration of the mainstem estuary, which is otherwise maintained at some low, background concentration.

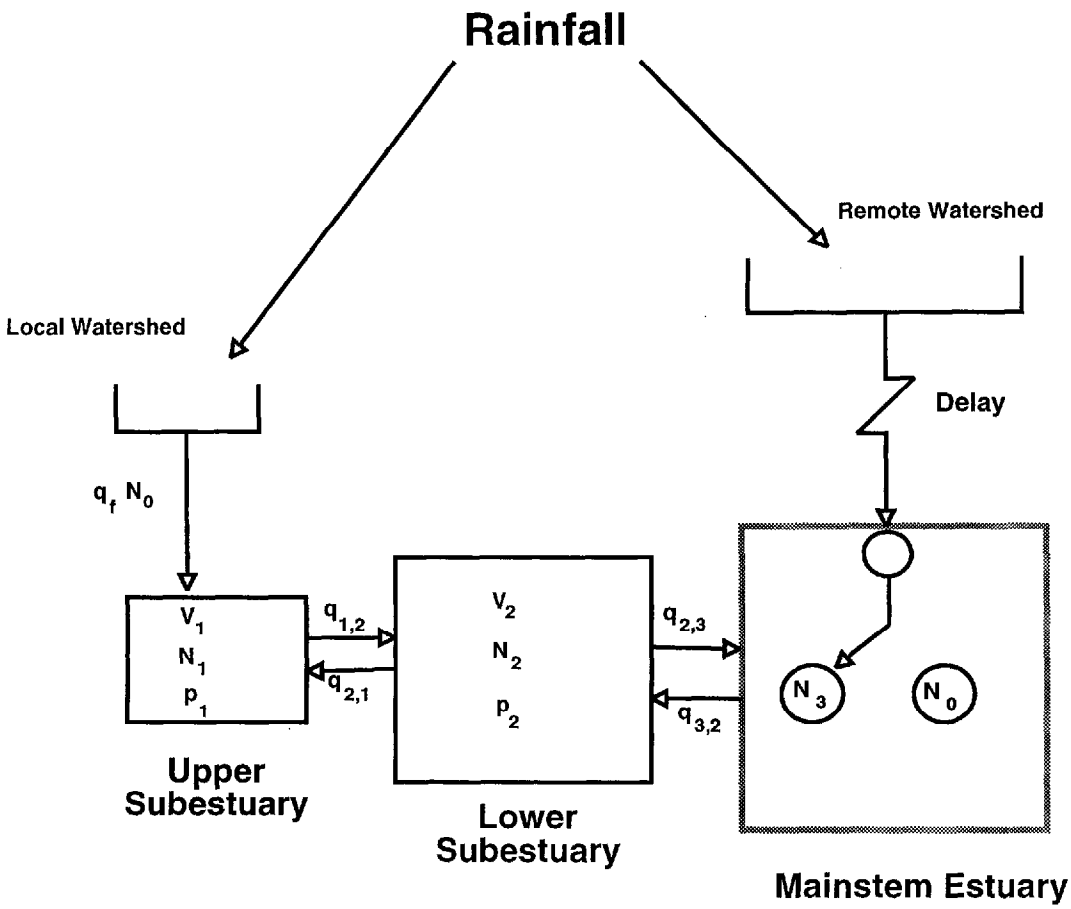

Fig. 1. Schematic representation of subestuary, consisting of two segments: an upper one receives direct runoff from the local watershed; the lower segment exchanges water with the upper and the mainstem estuary. A major runoff event adds nutrients directly to the upper segment and raises the concentration of nutrients in the mainstem estuary from N_3 to N_0 after a delay.

Mixing volumes for baseflow were chosen to exchange 38% of the volume of the upstream box and 25% of the downstream box per day, similar to previous box models of the Rhode River (Han 1974; Jordan et al. 1991*a*). Outward mixing coefficients vary with freshwater inflow, thereby conserving box volume under both baseflow and storm conditions. Upon the arrival of a simulated pulse on the mainstem estuary the mixing coefficient at the downstream boundary of the downstream box is increased to 75% d^{-1} to simulate the rapid exchange—induced by the two-layered flow and rapid exit of denser water from the subestuary—set up by the arrival of lighter, fresher water at the river mouth (Han 1974; Schubel and Pritchard 1986). We further assume that a period of diminished mixing follows the injection of nutrients from the mainstem, as would occur when salinity gradients are broken down (Schubel and Pritchard 1986).

Our intent is to model general patterns of phytoplankton biomass that might occur due to the inputs of nutrients from local and remote sources for an idealized subestuary. We use morphometric data and previously determined average mixing conditions for the Rhode River as guidance in choosing realistic, though not necessarily typical, values of these parameters.

Nutrients and phytoplankton—We model phytoplankton standing crop with a dynamic version of the model of Wofsy (1983),

Notation

N_u, N_0, N_3	NO_3^- concentration in segment j, in the influent freshwater, and in the downstream boundary segment, μg-atoms liter^{-1}
p_j	Phytoplankton biomass concentration in segment j, μg Chl liter^{-1}
$p_{s,j}$	Steady state concentration of phytoplankton biomass in segment j, μg Chl liter^{-1}
V_j	Volume of segment j, m^3
$q_{i,j}$	Volumetric exchange of water from segment i to j, m^3 d^{-1}
q_f	Volumetric inflow of freshwater, m^3 d^{-1}
k_c	Spectral mean absorption coefficient of phytoplankton, m^2 (mg Chl)$^{-1}$
k_d	Spectral mean absorption coefficient of phytoplankton-derived detritus, m^2 (mg Chl)$^{-1}$
k_t	Diffuse attenuation coefficient of inorganic suspended solids, m^{-1}
k_w	Diffuse attenuation coefficient due to water and dissolved substances, m^{-1}
Γ	Maximal specific growth rate of phytoplankton, d^{-1}
$r_0(N_j, K_n)$	Loss rate of phytoplankton due to grazing plus senescence as a fraction of Γ
r_{min}	Minimal value of r_0 approached as $N_j \to \infty$
r_{max}	Maximal value of r_0 at $N_j = 0$
K_n	Characteristic nutrient concentration which allows the growth of grazing-resistant phytoplankton species, μg-atoms liter^{-1}
I_0	Surface incident irradiance, quanta m^{-2} d^{-1}
I_k	Characteristic irradiance for the onset of light saturation, quanta m^{-2} d^{-1}
L	Sunlit fraction of the day
Z_0	Depth of the mixed layer, m
θ	Chl : N ratio of phytoplankton, μg Chl (μg-atoms N)$^{-1}$
τ_j	Time constant for adjustment of phytoplankton biomass concentration in segment j, d
μ_{avg}	Cosine of refracted solar zenith angle averaged over L

which predicts steady state phytoplankton biomass in a well-mixed, nutrient-saturated mixed layer. We base this approach on two observations: first, the Rhode River is eutrophic, with chlorophyll concentrations during spring and summer averaging 30–50 μg liter^{-1} in the lower subestuary; second, dissolved NH_4^+ is always present at background concentrations of 3–5 μg-atoms liter^{-1} (Jordan et al. 1991*a*). Even though the NH_4^+ may be saturating for growth rate, it is obvious from mass balance that production of significant amounts of new biomass requires input of new nutrients, as explained below.

The model incorporates the following four assumptions. High NH_4^+ is maintained by high regeneration rates that impose a high loss rate on the phytoplankton population. Regeneration is not modeled explicitly; the only requirement on the mechanism for regeneration is that it return nutrient to the water column rapidly. Microzooplankton grazing is a likely cause of regeneration (e.g. *see* Gallegos 1989; Dolan and Gallegos 1992). Blooms are initiated by input of (new) nutrients from external (i.e. local watershed or mainstem estuary) sources. We assume that increased nutrient inputs alter the short-term balance between growth and loss rates, allowing biomass to accumulate. The bloom assemblage is unable to grow and begins to dissipate when the added nutrient is depleted by the combined action of phytoplankton uptake and flushing. The mechanism of bloom demise is not specified; possible mechanisms include encystment, sedimentation, scenescence, and lysis. The externally supplied nutrient is sequestered by the crashing bloom population; i.e. the bloom-producing nutrient is not recycled on the longer time scales considered by the model.

The equations for phytoplankton growth and nutrient uptake (list of notation and Table 1) model the net source term for phytoplankton biomass, p as first-order approach to steady state (Eq. 1–4), where the steady state biomass p_s and the rate constant τ are given by equations 9 and 13 of Wofsy (1983) and reproduced here as Eq. 5 and 8. Note that equation 13 of Wofsy (1983) contains a typographical error in which an outer set of brackets was omitted; the expression in Table 1 is correct. Steady state biomass is not a constant, but rather is a moving target that the system is always approaching.

As summarized by Howarth (1988), growth rate of the species assemblage present at any time may be nutrient saturated, but *net* potential primary productivity of the system is still nutrient limited if nutrient enrichment causes shifts in species domi-

Table 1. Equations for nutrient concentration and phytoplankton biomass used to model bloom formation and dissipation in a subestuary.

$$\frac{dp_1}{dt} = \frac{1}{V_1}[q_{2,1}p_2 - (q_{2,1} + q_f)p_1] + \frac{1}{\tau_1}(p_{s,1} - p_1) \tag{1}$$

$$\frac{dp_2}{dt} = \frac{1}{V_2}[-q_{2,1}p_2 + (q_{2,1} + q_f)p_1 + (q_f + q_{2,3})(p_3 - p_2)] + \frac{1}{\tau_2}(p_{s,2} - p_2) \tag{2}$$

$$\frac{dN_1}{dt} = \frac{1}{V_1}[q_f N_0 + q_{2,1}N_2 - (q_f + q_{2,1})N_1] - \frac{1}{\tau_1}\frac{(p_{s,1} - p_1)}{\theta} \tag{3}$$

$$\frac{dN_2}{dt} = \frac{1}{V_2}(q_{3,2}N_3 - q_{2,3}N_2 + q_{1,2}N_1) - \frac{1}{\tau_2}\frac{(p_{s,2} - p_2)}{\theta} \tag{4}$$

$$p_{s,j} = \frac{1}{k_c + k_d}\left\{\frac{f\left(\frac{I_0}{I_k}\right)}{Z_0(j)r_0(N_j, K_n)} - [k_l(j) + k_w(j)]\right\} \tag{5}$$

$$f\left(\frac{I_0}{I_k}\right) = \mu_{avg}L \times \ln\left(\frac{2.7I_0}{I_k}\right) \tag{6}$$

$$r_0(N_j, K_n) = \frac{r_{max} + r_{min}\left(\frac{N_j}{K_n}\right)}{\left(\frac{N_j}{K_n}\right) + 1} \tag{7}$$

$$\tau_j = \left\{\Gamma r_0(N_j, K_n)\left[1 - \frac{r_0(N_0, K_n)Z_0(k_l + k_w)}{f\left(\frac{I_0}{I_k}\right)}\right]\right\}^{-1} \tag{8}$$

nance. To implement the assumption of bloom initiation by external nutrient inputs therefore requires that only r_0, the ratio of loss rate to growth rate, be a function of nutrient levels. That is, relationships of growth rate to nutrient concentration, whether intracellular or in the bulk medium, need not be explicitly considered.

The functional form of Eq. 7 (Fig. 2) was chosen empirically to summarize compactly the net effect of nutrient enrichment seen in more elaborate microplankton food-web models (e.g. Thingstad and Sakshaug 1990; *see discussion*). We sought a function with the characteristics $r_0 = 0.1$ as $N \to \infty$, and $r_0 = 0.6$ at $N = 0$. That is, at high nutrient concentrations we assume that the community consists of species that are not grazed and respiratory loss rates are 10% of maximal growth rates, consistent with observations on many phytoplankton cultures (Parsons et al. 1984). When external nutrients are exhausted the total fractional loss rate increases above that due to respiration alone because the nutrient-saturated condition is presumed to be maintained by regeneration; at steady state the system therefore supports a lower phytoplankton standing crop (Fig. 2).

Results of simulations—The system of equations (Table 1) was solved with a fourth-order Runge-Kutta numerical integration. Steady state solutions agreed with the analytical solution to at least six significant digits. Simulated concentrations of chlorophyll in the two boxes prior to influx of

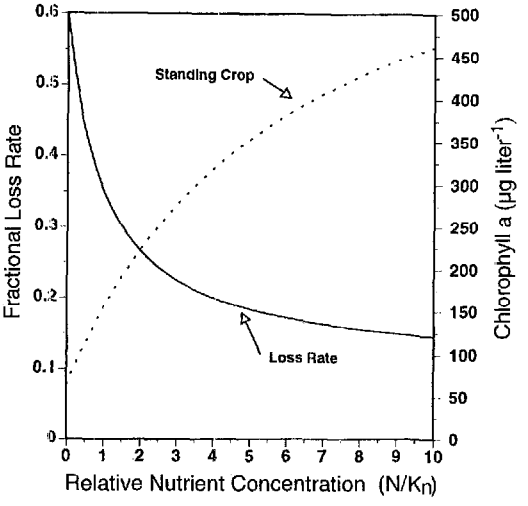

Fig. 2. Empirical function used to model phytoplankton fractional loss rate (r_0, Eq. 7) as a function of relative nutrient concentration, and the resulting maximal phytoplankton standing crop (Eq. 5).

nutrients (Fig. 3), with parameters given in Table 2, agree with summer averages for the upper and lower segments of the Rhode River subestuary. The simulated pulse of runoff from the local watershed raises the nutrient concentration in the upper segment to 15 µg-atoms liter^{-1}, but causes only an imperceptible rise in the concentration of the lower segment. Chlorophyll concentration in the upper segment responds rapidly with a short-lived bloom of ~80 µg liter^{-1}. Response to the local influx dissipates within 5 d, and there is no response in the lower segment.

The arrival of the pulse on the mainstem estuary, modeled as a delayed, 12-d rise in nutrient concentration at the boundary, results in increases in simulated nutrient concentration in both the lower and upper segments; in each segment, however, the highest nutrient concentrations achieved are lower than the maximal concentration in the upper segment in response to local input. By contrast, the simulated chlorophyll concentrations were higher in each segment than the maximal concentration achieved in response to local input, reaching a peak of ~105 µg liter^{-1}. The higher chlorophyll concentrations are the result of the longer duration of nutrient influx from the mainstem.

Table 2. Parameters, boundary conditions, and initial conditions used to simulate phytoplankton blooms with Eq. 1–8 of Table 1. (Units given in list of notation.)

	Value		Value
Biological parameters		Physical parameters	
k_c+k_d	0.016	V_1	1.3×10^5
Γ	1.25	V_2	6.5×10^6
r_{min}	0.10	$Z_0(1)$	1.0
r_{max}	0.60	$Z_0(2)$	2.0
I_0	1.81×10^{25}	$k_l+k_w(1)$	1.0
I_k	3.61×10^{24}	$k_l+k_w(2)$	0.60
μ_{avg}	0.81	Initial conditions	
L	0.58	N_1	0.0
$f(I_0/I_k)$	1.22	N_2	0.0
K_n	2.50	p_1	46.8
θ	0.40	p_2	37.1
Boundary conditions and variable forcing functions			
N_0	40.0	Constant	
N_3	2.5	Background	
	40.0	Day 17–29	
p_3	10.0	Constant	
q_f	5×10^3	Background	
	2×10^6	Day 5	
$q_{2,1}$	5×10^3	Constant	
$q_{1,2}$	$q_f+q_{2,1}$	Background and day 5	
$q_{3,2}$	1.625×10^6	Background	
	4.875×10^6	Day 17	
$q_{2,3}$	$q_f+q_{2,3}$	Background and day 5	

Results of the simulation suggest that the influence of the local watershed, given the morphology assumed here, should be restricted to the upstream segments. The bloom produced in response to simulated influx of nutrient from the local watershed was relatively short lived. In practice, it is likely that routine weekly or biweekly sampling schemes would miss most of the responses to local inputs. The longer lived and spatially more extensive blooms produced by arrival of the nutrient pulse from the mainstem would presumably be easier to detect with weekly sampling.

Study site and methods

Site—The Rhode River estuary (38°52′N, 76°32′W, Fig. 4) is one of several tributary embayments, or subestuaries, on the western shore of Chesapeake Bay in Maryland. It is 550 ha in area and averages 2 m deep with a maximum of 4 m. The mean tidal range is 30 cm, but weather often causes

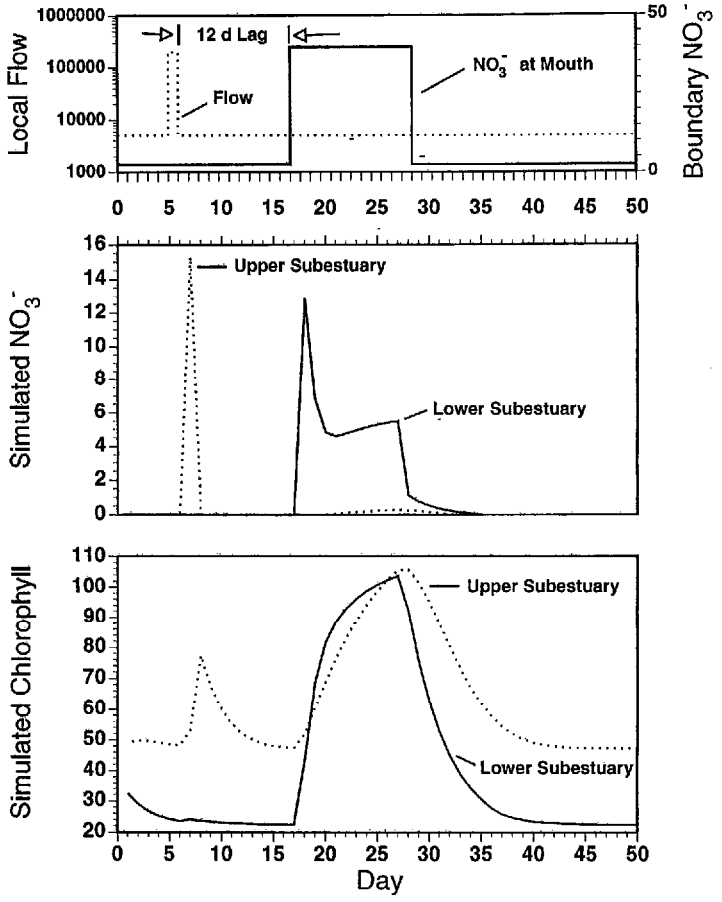

Fig. 3. Simulated pulse of runoff from the local watershed (m^3 d^{-1}, upper panel, dotted line) results in a sharp rise in NO_3^- concentration in the upper subestuary (μg-atoms $liter^{-1}$, middle panel, dotted line) and a short-lived bloom (μg $liter^{-1}$, lower panel, dotted line) peaking on day 9. Arrival of the freshet on the mainstem estuary raises the NO_3^- concentration at the lower boundary (upper panel, solid line) and lower subestuary (middle panel, solid line), and results in blooms in both segments.

more extreme changes in water level. Salinity varies seasonally from 0‰ at the head of the estuary in spring to almost 20‰ at the mouth in fall during years with low runoff. Mixing in most of the Rhode River, as in many subestuaries of Chesapeake Bay, is driven by changes in salinity in the Chesapeake Bay (Han 1974; Schubel and Pritchard 1986).

The 2,300-ha watershed of the upper estuary (Fig. 4) is 63% forest, 18% crop land, 13% pasture, and 7% residential. The upper estuary includes 23 ha of shallow mudflat and creek areas bordered by 12 ha of low marsh and 22 ha of high marsh. Mudflats and creeks are exposed by $<1\%$ of the low tides and are, thus, essentially subtidal.

Automated monitors—We measured daily precipitation with a rain gauge located at a central weather station on the Rhode River watershed. Discharge from up to 90% of the watershed of Muddy Creek, the principal freshwater source to the Rhode River, was monitored with a network of weirs and automated samplers (Fig. 4). Flow was measured at V-notch weirs, and samples in volumes proportional to the flow were pumped into acid-washed glass carboys (Correll 1981). Samples were composited weekly and analyzed for total N, P, organic C, PO_4^{3-},

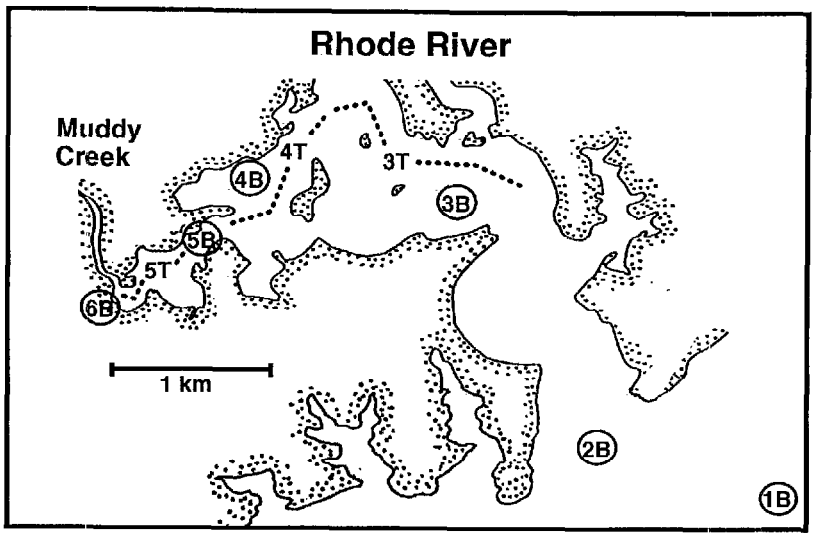

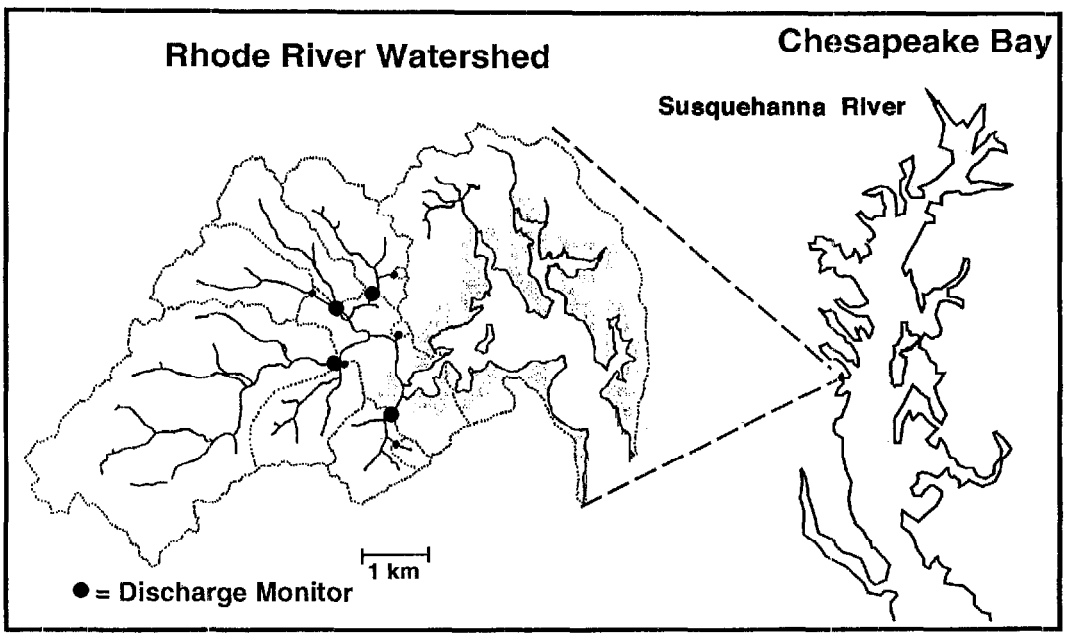

Fig. 4. Map of Rhode River showing location on Chesapeake Bay, watershed boundaries, and automated monitors (lower panel) and estuarine sampling locations (upper panel). Station numbers ending in "T" designate transect (pump) samples; those ending in "B" designate stations sampled by bottle cast. Watershed Sta. 122 is coincident with Sta. 5B.

NO_3^-, and NH_4^+. Here we focus exclusively on NO_3^- influx.

As an indicator of timing and relative magnitude of week-to-week variations in NO_3^- influx from the local watershed, we summed the inputs from four second- or third-order streams (Fig. 4) representing 36% of the watershed of Muddy Creek. The station that monitors most of the remaining watershed is tidally influenced, complicating the calculation of mass influx. We calculated mass influx by multiplying flow-weighted NO_3^- concentration by volumetric flow for each station and summing over the four stations. Land use in the subwatershed with tidally influenced monitors is a combination of uplands and swamps, so that the inputs reported probably represent a fraction slightly >36% of total influx.

For selected weeks, NO_3^- concentrations were available from an automated station at the downstream end of the mudflat in the tidal creek (Sta. 122, Correll 1981). This station measured tidal exchange between the intertidal zone and the estuarine basin at a point where the width of the creek is constricted to 165 m but still has a depth of only ~1 m at MLW. The station consisted of an instrument shed on pilings and was equipped with an electromagnetic current meter (Marsh-McBirney model 711) and an electronic interface that integrated water flux over time. Samples proportional to flow were pumped every 30 min into separate carboys for ebbing and flooding tides.

Flow data for the Susquehanna River were measured at the Conowingo Dam near the mouth of the river. These data were made available by the U.S. Geological Survey.

Field sampling and analytical methods—We divided the Rhode River subestuary into eight numbered segments with lengths greater than a tidal excursion and boundaries corresponding to constrictions in the width of the estuary (Fig. 4). Samples for phytoplankton chlorophyll, species composition, and photosynthesis-irradiance curves were collected along a transect of seven stations from 1.4 km downstream to 5.5 km upstream of the mouth of the river (Fig. 4). Samples were collected from the Secchi depth with a 2-liter Labline Teflon sampler, emptied into 2-liter polyethylene containers (shielded from direct sunlight), and returned to the laboratory in a cooler. Cruises were generally conducted weekly; we sampled daily during a 7-d period following a local storm in July 1989. Stations sampled for phytoplankton are indicated by a number representing the segment of the river followed by the letter "B" denoting bottle cast.

Subsamples for chlorophyll analyses were filtered onto Whatman GF/F glass-fiber filters immediately upon return to the laboratory. Filters were extracted in 10 ml of 90% acetone overnight at 4°C either immediately or after freezing for <2 weeks. Extracted chlorophyll was estimated fluorometrically with a Gilson Spectra-Glo fluorometer calibrated against Chl *a* determined periodically with the spectrophotometric equations of Jeffrey and Humphrey (1975). Species composition and photosynthesis data are reported elsewhere (Gallegos 1992).

Samples for nutrient analyses were collected on separate cruises at approximately biweekly intervals. Spatially integrated samples were collected by continuously pumping water from a depth of 10 cm while cruising the lengths of the segments. NO_3^- concentrations were determined after filtration (prewashed 0.45-μm Millipore), reduction to NO_2^- by Cd amalgam, and reaction with sulfanilamide (Am. Public Health Assoc. 1976). Locations of nutrient samples are designated by a segment number followed by the letter "T" denoting a pumped transect sample.

Results

Two rainy periods during late spring and early summer of 1989 elevated the inputs of NO_3^- from the local watershed. These runoff events were followed by brief blooms in the upper subestuary in the regions of Sta. 6B and 5B. The storms were large enough in areal extent to produce an elevated hydrograph on the Susquehanna River. Arrival of the increased Susquehanna flow from the first event was detected as a drop in salinity throughout the Rhode River after a lag of ~12 d. Nutrient inputs from

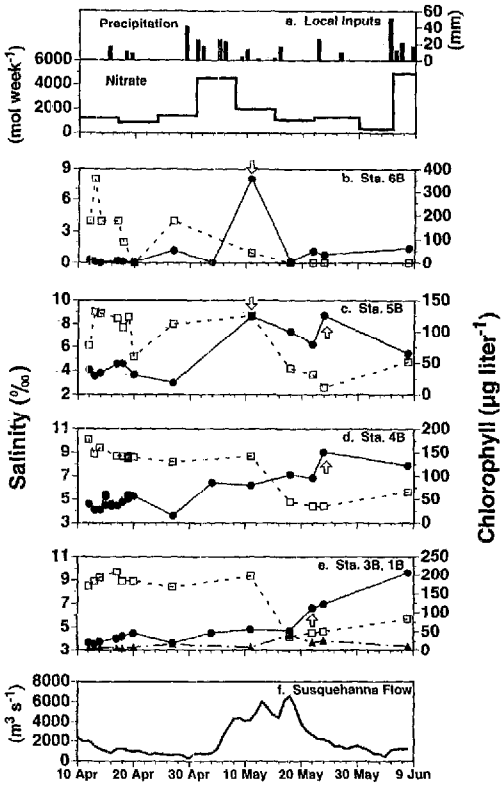

Fig. 5. [a.] Local precipitation (bars) and weekly NO_3^- input (steps) from the gauged subwatersheds of Muddy Creek, 10 April–9 June 1989. [b–e.] Response of salinity (□) and chlorophyll concentrations (●) along the axis of the Rhode River from the upper subestuary (b,c) to lower subestuary (d,e) stations. Downward arrows indicate response to local inputs; upward arrows indicate response to remote inputs. Triangles in panel e show chlorophyll concentration at Sta. 1B, 1.4 km beyond mouth of the Rhode River. [f.] Flow of the Susquehanna River at Conowingo dam.

the arrival of elevated Susquehanna flows caused blooms throughout the Rhode River. For clarity we present the sequence of events for each period separately, but in fact, the bloom resulting from the arrival of the first pulse from the Susquehanna was long lived and became part of an unusually high background chlorophyll concentration for the second pulse.

10 April–9 June 1989—A period of rainfall during late April and early May 1989 resulted in elevated NO_3^- loading for the week of 1–8 May (Fig. 5a). Salinity at Sta. 6B, the mouth of Muddy Creek, declined due to the local runoff, reaching 0‰ on 18 May, where it remained through mid-June (Fig. 5b). Chlorophyll concentration at Sta. 6B was depressed on 4 May due to washout by the freshwater discharge (Fig. 5b). The following sampling day (13 May) we observed a bloom of ~350 µg Chl liter^{-1} at this station, which was short lived due to washout by subsequent storms (Fig. 5b).

NO_3^- at the upper estuary transect, Sta. 5T, increased from 0.3 to 4.9 µg-atoms liter^{-1} between 27 April and 11 May (Table 3), even though salinities at Sta. 5B showed no response to the local inputs (Fig. 5c). Chlorophyll concentration at Sta. 5B was elevated on 11 May, declined over the next two sampling days, and rose again on 24 May.

Neither salinities at the bottle-cast Sta. 3B and 4B (Fig. 5d,e) nor the NO_3^- concentrations in the lower subestuary transects measured on 11 May (Table 3, Sta. 3T and 4T) showed any response to the elevated inputs measured at the stream weirs from 1–8 May. Between 11 and 18 May, however, salinities at Sta. 5B, 4B, and 3B declined by 4–5‰ (Fig. 5b–d). Comparing the salinity drop with flow of the Susquehanna River at Conowingo Dam, which began to rise on 6 May (Fig. 5e), suggests a lag of ~12 d for arrival of the freshet at the Rhode River. On 22 May the NO_3^- concentration was elevated throughout the subestuary (Table 3); the highest concentrations were observed at the most downstream segment sampled, indicating influx of NO_3^- with arrival of the freshwater. NO_3^- concentration measured during the previous week at the tidal flux station, 122, was higher than that measured farther upstream in the transect sample, 5T, which would be expected whenever the source of NO_3^- is the mainstem estuary.

For 2 weeks preceding the drop in salinity, chlorophyll concentrations in the lower subestuary at Sta. 3B and 4B were at levels (50–90 µg liter^{-1}) typical for the spring bloom at those locations (Fig. 5d,e; cf. figure 3, Jordan et al. 1991*a*). Coincident with the drop in salinity, chlorophyll concentration began to rise, first at the outer station, 3B, then at 4B. Chlorophyll concentration at Sta. 1B, where the Rhode and West Rivers join

Table 3. Dissolved NH_4^+ and NO_3^- ($+NO_2^-$) concentrations (μg-atoms liter^{-1}) measured in spatially integrated (Sta. 3T, 4T, and 5T), and NO_3^- ($+NO_2^-$) concentrations in weekly integrated samples from the tidal flux station (Sta. 122). Values for Sta. 122 are averages of ebbing and flooding samples, except as noted. Data for first and second bloom periods are, respectively, above and below dashed line.

	Sta. 3T		Sta. 4T		Sta. 5T		Sta. 122
Date	NH_4^+	NO_3^-	NH_4^+	NO_3^-	NH_4^+	NO_3^-	NO_3^-
7–24 Apr							0.3
27Apr	3.4	0.9	1.3	0.3	1.3	0.3	
24 Apr–1 May							1.1
11 May	2.4	0.1	2.2	0.1	2.4	4.9	
15–22 May							9.7
22 May	3.6	24.9	3.8	15.7	2.5	5.6	
22–30 May							4.8
30 May–5 Jun							1.9
8 Jun	3.6	2.8	1.6	3.5	12.6	8.0	
5–12 Jun							1.6
12–19 Jun							3.6
22 Jun	5.7	0.3	4.4	0.2	8.7	5.4	
19–26 Jun							0.9
26 Jun–3 Jul							1.1
3–10 Jul*							157.8
11 Jul	3.9	1.2	2.9	0.3	2.6	0.4	
10–17 Jul							3.0

* Total sample pumped into floodtide container due to bias in current meter.

Chesapeake Bay (Fig. 5e, triangles) was elevated on 18 May and nearly equal to that at Sta. 3B. Thus chlorophyll-rich water arrived with the NO_3^--rich freshet, but chlorophyll concentration still increased with distance upstream, indicating no *net* import of chlorophyll. Peak concentrations at the lower subestuary stations may have been missed due to a gap in sampling, but on 8 June chlorophyll concentrations remained as high as 180 and 120 μg liter^{-1} at Sta. 3B and 4B (Fig. 5e,d).

4 June–24 July—A rainy period from 4 to 24 June 1989 led to 3 weeks in which NO_3^- loading from the four local subwatersheds ranged from 2 to 5 $\times$ 10^3 mol week^{-1} (Fig. 6a). Salinity at Sta. 6B (Fig. 6b), which had recovered to 4‰ on 12 June, declined to 0‰ again on 19 June, where it remained through the rest of the observation period. Chlorophyll concentration at Sta. 6B rose to ~250 μg liter^{-1} on 19 June, then declined steadily due to washout by the local discharge (Fig. 6b).

NO_3^- concentrations measured on 22 June (near the end of the rainy period) were low in the lower subestuary and high (>5 μg-atoms liter^{-1}) in the upper subestuary (Table 3). Although the decline in salinity between 12 and 19 June was slight (Fig. 6c), the lower NO_3^- concentration measured during the preceding week at the tidal flux station together with the observation that NO_3^- increased in the upstream direction on 22 June suggest that the source of the elevated NO_3^- concentration at transect Sta. 5T was local runoff. Chlorophyll concentration at Sta. 5B peaked at ~500 μg liter^{-1} on 20 June and declined over the next 2 sampling dates (Fig. 6c). After a 10-d period without rain, a more intense storm on 5–6 July resulted in the highest NO_3^- loading from the local watersheds (Fig. 6a), the highest NO_3^- concentration at the tidal flux station (Table 3), and the highest chlorophyll concentrations (Fig. 6b) that were observed during spring and summer.

In response to the rainy period, flow of the Susquehanna River showed a broad 2-week rise beginning on 15 June (Fig. 6f), but peak flows and the duration of elevated flows fell below those of the earlier event. Arrival of the pulse at the Rhode River was difficult to detect, but the high chlorophyll at Sta. 1B (Fig. 6d) on 27 June suggests that the slight decrease in salinity at Sta. 3B on that date was probably due to the Susquehanna flow. The water-quality transect sam-

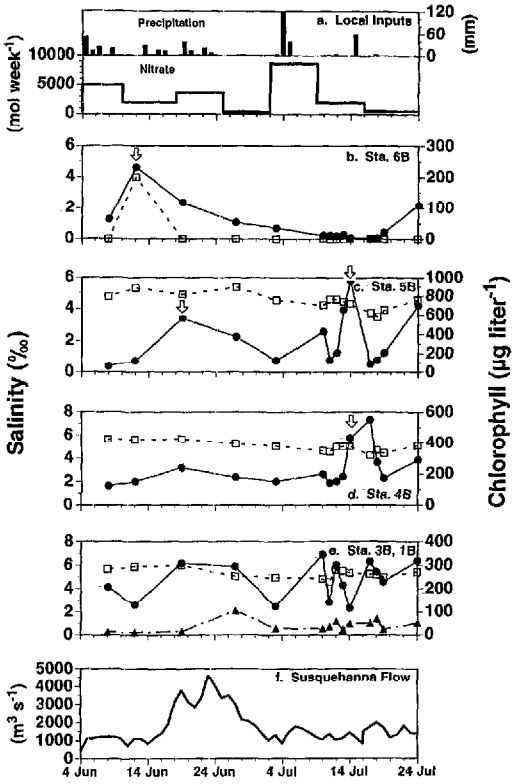

Fig. 6. As Fig. 5 but for 4 June–24 July 1989. Note changes in scale.

pling was too infrequent to detect any NO_3^- influx, had there been any.

Chlorophyll concentrations in the lower subestuary Sta. 4B and 3B (Fig. 6d,e) were at very high levels throughout June. Variations at Sta. 3B were erratic, and concentrations at Sta. 4B, prior to the local event of 5–6 July, were relatively constant. At neither station in the lower subestuary was there a well-defined response attributable to the arrival of the flow pulse from the Susquehanna River, suggesting that NO_3^- was depleted before arrival at this site and (or) that the volume of water exchanged was minimal. The chlorophyll concentrations were, however, well above the 30–50 μg liter^{-1} and salinity well below the 8–9‰ seasonal averages for these segments (*see* figures 3 and 2, Jordan et al. 1991*a*). The influx of 27 June may, therefore, have prolonged the response to the NO_3^- influx and elevated baseflow that followed the mid-May flow pulse.

Discussion

Comparison of model and field results—The model used to simulate the response of phytoplankton biomass to nutrient inputs from the local and remote watersheds is a highly simplified representation of both the physical and biological processes governing nutrient fluxes and phytoplankton dynamics in a subestuary. Its simplicity, however, facilitates its use in examining certain features of the interaction between watersheds and receiving waters. The blooms produced in response to the simulated influx of nutrients exhibited spatial patterns in response to local and remote inputs that, in certain respects, resembled the field data but differed in other important ways.

In the model, inputs from the local watershed produced short-lived blooms in the upper segment, and simulated arrival of water with elevated nutrient concentration at the seaward boundary produced blooms throughout the subestuary (Fig. 3). In the field data, responses to local and remote inputs can be discerned in spring (Fig. 5), but permanently assigning the sampling locations to "upper subestuary" and "lower subestuary" compartments is tenuous. For example, the high chlorophyll concentration at Sta. 6B on 11 May (Fig. 5B), which may have been a localized patch, appeared to be a response to local nitrogen inputs, but chlorophyll was flushed away from Sta. 6B by subsequent runoff until mid-June, when roughly the same sequence of bloom followed by washout was repeated.

In spring, chlorophyll concentrations at Sta. 5B bore some resemblance to the model results for the upper subestuary, responding to both local and remote inputs; blooms at Sta. 4B and 3B were initiated only after the salinity drop due to the arrival of the freshet from the Susquehanna River, similar to the lower subestuary segment in the model. In summer, however, peak flow and duration of the runoff of the Susquehanna River were less than in spring, and arrival of the freshet at the Rhode River was indicated by a rise in chlorophyll at Sta. 1B and only a minor

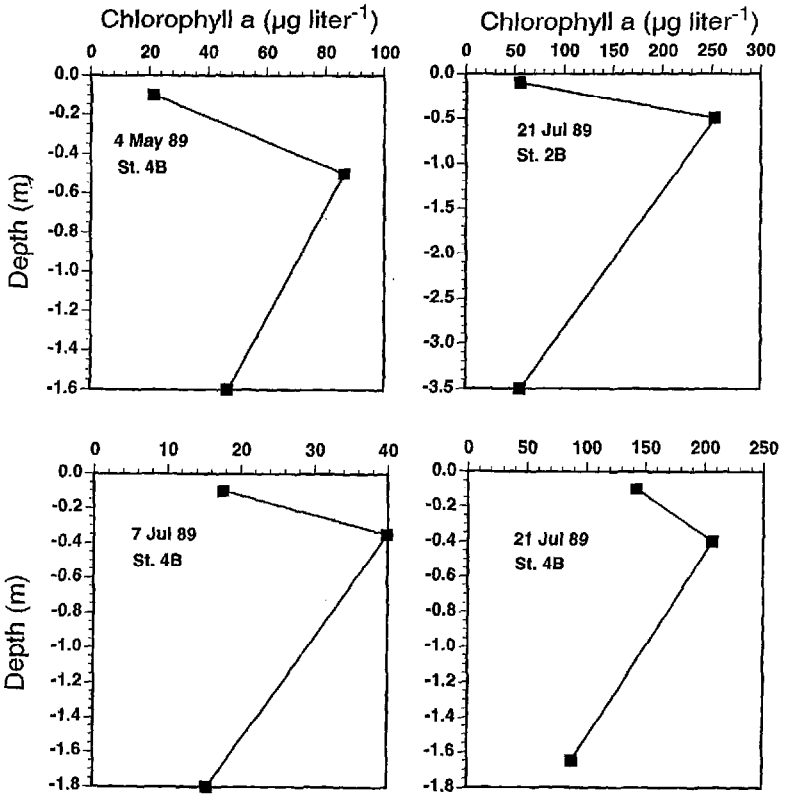

Fig. 7. Depth profiles of chlorophyll showing subsurface maxima measured during blooms on the Rhode River.

drop in salinity at Sta. 3B. Furthermore, latitudinal distributions of NO_3^- for the main Chesapeake Bay in 1989 (Magnien et al. unpubl. data rep.) showed substantial reduction in the southerly direction in June and July but not in May. Obviously, the mainstem estuary is an ecosystem with seasonal dynamics of its own; thus, the delivery of nutrients to a subestuary from the mainstem can be expected to occur only when physical process in the mainstem (e.g. some combination of flow, temperature, daylength, turbidity, mixing depth) limit biological utilization of the nutrients before arrival at the subestuary. Litaker et al. (1987) observed similar seasonal differences in the response of nutrient loading to weather systems in the Newport River estuary in North Carolina.

The blooms simulated by the model were of much smaller magnitude than those observed during early and midsummer 1989. We believe that much of the difference between simulated and observed bloom levels is due to depth variation of the phytoplankton biomass. On several occasions in connection with measurement of underwater irradiance spectra (Gallegos et al. 1990) we measured chlorophyll at three depths, i.e. near-surface, near-bottom, and at the Secchi depth (Fig. 7). Subsurface maxima were frequently observed in the sample from the Secchi depth. The ability of the organisms to form subsurface biomass peaks will adversely affect the correspondence of simulated and observed chlorophyll concentrations in at least two ways. First, the sample from the Secchi depth may overestimate the depth-integrated value by a factor of 2–3. Second, for organisms able to maintain a

preferred depth stratum, Z in the model will overestimate the depth over which the plankton are actually mixing, and hence the model will underestimate the nutrient-saturated standing crop (Eq. 5, Table 1). Finally, the elevated chlorophyll concentrations at the mouth of the Rhode River that arrived with the freshet, while not sufficient to result in net import of chlorophyll to the river, would reduce net export at the initiation of the bloom; this effect was not included in the model, but, if included, would increase the magnitude of simulated blooms by reducing simulated export losses and elevating initial chlorophyll values.

Bannister (1974) suggested that his equation for nutrient-saturated, steady state phytoplankton biomass in a mixed layer could be extended to include the nutrient-limited case and used for dynamic simulations, provided one knew how θ, the Chl : N ratio of phytoplankton, varied with time and (or) environmental conditions. Indeed, more recent models (e.g. Laws and Chalup 1990) of phytoplankton growth under light or nutrient limitation reveal many additional parameters of potential importance. The possibility of applying such models in a multispecies, dynamic environment remains elusive. A simple model amenable to sensitivity analysis and capable of forecasting the timing and location of blooms in relation to local and remote watershed inputs should prove most useful in mounting more intensive investigations of bloom formation and dissipation.

Nutrients and phytoplankton blooms—In discussions of blooms and eutrophication, it is nutrient limitation of net primary production that must be considered (Howarth 1988). Our treatment focuses on net primary production of biomass by altering only the *ratio* of loss rates to growth rate in response to allochthonous nutrient inputs.

Although it is not a mechanistic treatment, it is important that our simple formula for r_0 (Eq. 7) be consistent with results of more detailed models of the mechanisms believed to govern the composite parameter. The nutrient-flow model of a microplankton food web by Thingstad and Sakshaug (1990) contains many of the attributes needed to evaluate the simple formulation of r_0 used here. Their model of a closed food web (i.e. no sedimentation losses or allochthonous inputs) considers two size fractions of autotrophs, with the larger size fraction having lower nutrient affinity and lower maximal growth rate than the smaller fraction. Their simulations of the effects of increasing total nutrient enrichment on food-web structure demonstrate that the larger size fraction of autotrophs becomes established only after the smaller size fraction is nutrient saturated and residual free nutrient concentration increases. Furthermore, they showed that the larger size fraction does not become established until its growth rate is at or near its maximum; the long food chain supported by the increased enrichment limits grazing losses of the larger size fraction, allowing net increase of autotrophic biomass. Thus, our simple equation for r_0 as a function of nutrient enrichment reproduces essential features of a more elaborate model.

Residual NH_4^+ in the Rhode River is well above the total nutrient content considered in the simulations by Thingstad and Sakshaug (1990), supporting our contention that growth rate of a background phytoplankton assemblage in the Rhode River is at all times nutrient saturated. Interestingly, Pennock (1985) found that chlorophyll concentrations in the Delaware estuary during spring and fall blooms were correctly predicted by Wofsy's (1983) model, but that summer levels were overestimated despite nonlimiting nutrients. He hypothesized that summer biomass was regulated by a combination of light and grazing but did not attempt to better predict summer biomass levels by elevating r_0 above its basal value of 0.1.

Plankton dynamics in the land margin—Lewis and Platt (1982) gave a theoretical background for determining the relevant time scales over which the biological dynamics in an estuary may be considered functionally autonomous with respect to physical forcing by water motions on the continental shelf. Similar to the cases they analyzed, the dynamics of phytoplankton biomass throughout most of the Rhode River are governed by exchange of water masses with surface waters of the seaward boundary, i.e. Chesapeake Bay. Strong salinity gra-

dients induced by the arrival of a freshet down the main axis of the bay appeared to inject nutrients rapidly into the Rhode River, but subsequent decline in exchange rates and salinity gradients are necessary to account for bloom formation in the Rhode River.

In a subestuary such as the Rhode River, the seaward boundary is another estuary. The water driving the exchange across the boundary of the subestuary is, therefore, subject to complex interactions between its own watershed and plankton dynamics on both seasonal and event time scales (Malone et al. 1988; Loftus et al. 1972; and Figs. 5f, 6f herein). The result of the nesting of watersheds at the land margin is that single events can give rise to multiple responses in a subestuary. The timing and relative magnitude of the system's response to the local input as opposed to exchange across the mouth can be expected to vary with position of the subestuary along the main axis and with the order of the tributary. Thus on the Potomac River, a major tributary to the bay, Bennett et al. (1986) observed strong coupling of chlorophyll concentrations in the transition zone with flow events on the Potomac of 10–15-d duration. On the Rhode River, shorter term events were capable of producing blooms in the upper estuary (Figs. 5, 6), but the highest chlorophyll values of all were observed shortly after a major storm on the local watershed that was superimposed on a background biomass already much higher than the seasonal average.

Viewed in hierarchical perspective, these results suggest complex interactions in which qualitative and quantitative features of phytoplankton production in a subestuary depend on climatology and land use patterns at both local and regional scales. Considering the differences in nitrogen concentrations of runoff from cropland as opposed to forests (Correll 1981) and the role of riparian forests in removal of nitrogen from cropland runoff (Peterjohn and Correll 1984), it is easy to see that the magnitude and frequency of phytoplankton blooms potentially depend on both relative amounts and the spatial arrangements of the various land-use types locally and regionally. Further considering the effects of nutrient enrichment on food-web structure (Thingstad and Sakshaug 1990), a view emerges analogous to landscape ecology (e.g. Forman and Godron 1986) in which patterns and processes at small scales (e.g. microplankton community structure) depend on spatial arrangement and nutrient throughput of whole ecosystems on the watershed.

References

American Public Health Association. 1976. Standard methods for the examination of water and wastewater, 14th ed. APHA.

Bannister, T. T. 1974. A general theory of phytoplankton growth in a nutrient-saturated mixed layer. Limnol. Oceanogr. **19:** 13–30.

Bennett, J. P., J. W. Woodward, and D. J. Shultz. 1986. Effect of discharge on the chlorophyll *a* distribution in the tidally-influenced Potomac River. Estuaries **9:** 250–260.

Cloern, D. E. 1987. Turbidity as a control on phytoplankton biomass and productivity in estuaries. Cont. Shelf Res. **7:** 1367–1381.

Correll, D. L. 1978. Estuarine productivity. BioScience **28:** 646–650.

———. 1981. Nutrient mass balances for the watershed, headwaters, intertidal zone, and basin of the Rhode River estuary. Limnol. Oceanogr. **26:** 1142–1149.

Côté, B., and T. Platt. 1983. Day-to-day variations in the spring-summer photosynthetic parameters of coastal marine phytoplankton. Limnol. Oceanogr. **28:** 320–344.

Dolan, J. R., and C. L. Gallegos. 1992. Trophic coupling of rotifers, microflagellates, and bacteria during fall months in the Rhode River estuary. Mar. Ecol. Prog. Ser. In press.

Duda, A. M. 1982. Municipal point source and agricultural nonpoint source contributions to coastal eutrophication. Water Resour. Bull. **18:** 397–407.

Forman, T. T. T., and M. Godron. 1986. Landscape ecology. Wiley.

Gallegos, C. L. 1989. Microzooplankton grazing on phytoplankton in the Rhode River: Nonlinear feeding kinetics. Mar. Ecol. Prog. Ser. **57:** 23–33.

———. 1992. Phytoplankton photosynthesis, productivity, and species composition in a eutrophic estuary: Comparison of bloom and nonbloom assemblages. Mar. Ecol. Prog. Ser. **81:** 257–267.

———, D. L. Correll, and J. W. Pierce. 1990. Modeling spectral diffuse attenuation, absorption, and scattering coefficients in a turbid estuary. Limnol. Oceanogr. **35:** 1486–1502.

Han, G. C. 1974. Salt balance and exchange in the Rhode River, a tributary embayment to the Chesapeake Bay. Ph.D. thesis, Johns Hopkins Univ. 189 p.

Hayward, D., C. S. Welch, and L. W. Haas. 1982. York River destratification: An estuary-subestuary interaction. Science **216:** 1413–1414.

Howarth, R. W. 1988. Nutrient limitation of net

primary production in marine ecosystems. Annu. Rev. Ecol. Syst. **19:** 89–110.

HUTCHINSON, G. E. 1967. Eutrophication, past and present, p. 17–26. *In* Eutrophication: Causes, consequences, correctives. Natl. Acad. Sci.

JEFFREY, S. W., AND G. F. HUMPHREY. 1975. New spectrophotometric equations for determining chlorophyll *a, b,* c_1, and c_2 in higher plants, algae and natural phytoplankton. Biochem. Physiol. Pflanz. **167:** 191–194.

JORDAN, T. E., D. L. CORRELL, J. MIKLAS, AND D. E. WELLER. 1991*a*. Nutrients and chlorophyll at the interface of a watershed and an estuary. Limnol. Oceanogr. **36:** 251–267.

———, ———, ———, AND ———. 1991*b*. Long-term trends in estuarine nutrients and chlorophyll, and short-term effects of variation in watershed discharge. Mar. Ecol. Prog. Ser. **75:** 121–132.

LAWS, E. A., AND M. S. CHALUP. 1990. A microalgal growth model. Limnol. Oceanogr. **35:** 597–608.

LEWIS, M. R., AND T. PLATT. 1982. Scales of variability in estuarine ecosystems, p. 3–20. *In* V. S. Kennedy [ed.], Estuarine comparisons. Academic.

LIKENS, G. E. 1984. Beyond the shoreline: A watershed-ecosystem approach. Int. Ver. Theor. Agnew. Limnol. Verh. **22:** 1–22.

——— [ED.]. 1985. An ecosystem approach to aquatic ecology. Springer.

LITAKER, W., C. S. DUKE, B. E. KENNY, AND J. RAMUS. 1987. Short-term environmental variability and phytoplankton abundance in a shallow tidal estuary. 1. Winter and summer. Mar. Biol. **96:** 115–121.

LOFTUS, M. E., D. V. SUBBA RAO, AND H. H. SELIGER. 1972. Growth and dissipation of phytoplankton in Chesapeake Bay. 1. Response to a large pulse of rainfall. Chesapeake Sci. **13:** 282–299.

MALONE, T. C., L. H. CROCKER, S. E. PIKE, AND B. W. WENDLER. 1988. Influences of river flow on the dynamics of phytoplankton production in a partially stratified estuary. Mar. Ecol. Prog. Ser. **48:** 235–249.

OFFICER, C. B. 1980. Box models revisited, p. 65–114. *In* P. Hamilton and K. B. MacDonald [eds.], Estuarine and wetland process with emphasis on modeling. Plenum.

PAERL, H. W. 1988. Nuisance phytoplankton blooms in coastal, estuarine, and inland waters. Limnol. Oceanogr. **33:** 823–847.

PARSONS, T. R., M. TAKAHASHI, AND B. HARGRAVE. 1984. Biological oceanographic processes, 3rd ed. Pergamon.

PENNOCK, J. R. 1985. Chlorophyll distributions in the Delaware estuary: Regulation by light-limitation. Estuarine Coastal Shelf Sci. **21:** 711–725.

PETERJOHN, W. T., AND D. L. CORRELL. 1984. Nutrient dynamics in an agricultural watershed: Observations on the role of a riperian forest. Ecology **65:** 1466–1475.

RANDALL, J. M., AND J. W. DAY, JR. 1987. Effects of river discharge and vertical circulation on aquatic primary production in a turbid Louisiana (USA) estuary. Neth. J. Sea Res. **21:** 231–242.

SCHUBEL, J. R., AND D. W. PRITCHARD. 1986. Responses of upper Chesapeake Bay to variations in discharge of the Susquehanna River. Estuaries **9:** 236–249.

THINGSTAD, T. F., AND E. SAKSHAUG. 1990. Control of phytoplankton growth in nutrient recycling ecosystems. Theory and terminology. Mar. Ecol. Prog. Ser. **63:** 261–272.

VANNOTE, R. L., G. W. MINSHALL, K. W. CUMMINS, J. R. SEDELL, AND C. E. CUSHING. 1980. The river continuum concept. Can. J. Fish. Aquat. Sci. **37:** 130–137.

WOFSY, S. C. 1983. A simple model to predict extinction coefficients and phytoplankton biomass in eutrophic waters. Limnol. Oceanogr. **28:** 1144–1155.

Submitted: 27 December 1990
Accepted: 7 November 1991
Revised: 30 January 1992